

### 3. The Chilean Tsunami of May 24, 1960 at Amami-Ōshima.

By Takao MOMOI,

Earthquake Research Institute.

(Read Sep. 25, 1962.—Received Dec. 28, 1962.)

#### 1. Introduction

The Chilean Tsunami of May 24, 1960 which invaded Amami-Ōshima in the southern part of Japan caused very high waves in the central and the northern part of the island.

In this paper we have explained these extra-ordinarily high waves by use of a refraction diagram and the results of some numerical computations.

#### 2. Refraction Diagram around the Island

Contours are drawn every two hundred meters on the bathymetric

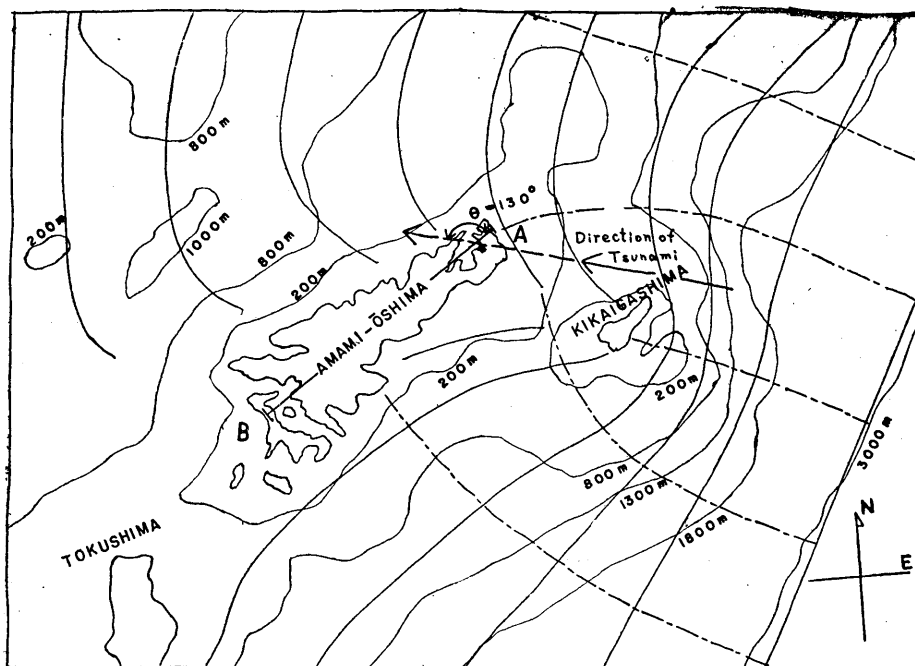


Fig. 1. Refraction diagram in the adjacent sea of Amami-Ōshima.

chart published by the Japanese Hydrographic Office. We draw fronts of the tsunami on the basis of Heugens' principle, supposing that the front of the tsunami at a depth of one thousand three hundred meters is nearly straight and travels with a velocity of long wave  $\sqrt{gH}$  ( $g$ : the acceleration of gravity,  $H$ : the depth of the sea). Whenever a criss-cross appears we cut off the waves behind the frontal wave. Figure 1 represents a refraction diagram which we obtain in this way.

### 3. Diffraction around the Island

For convenience of mathematical treatment we represented the island by a plate model AB (Fig. 1).

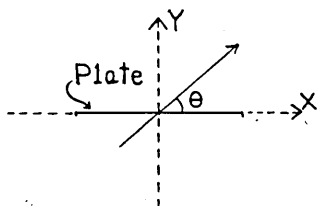


Fig. 2.

Referring to Fig. 2, a plane wave in water travels toward the origin from the lower side and impinges at an angle  $\theta$  on a plate-shaped island with the axis  $Z'OZ$ , normal to the plane of the paper. The island is immobile and non-absorbent. Its presence causes the wave to be fragmented.

The two-dimensional wave equation is (the case of vibration)

$$\left(\frac{\partial^2}{\partial x^2} + \frac{\partial^2}{\partial y^2} + k_1^2\right)\zeta = 0, \quad (1)$$

where  $\zeta$  is the elevation of water from the undisturbed free surface,  $k_1 = \omega/c$ , and  $c$  is the velocity of long wave in water or  $\sqrt{gH}$ .

We have two boundary conditions. The first boundary condition is that the sum of the fluxes of the incident and scattered waves vanishes at the surface of the plate. If  $\zeta_1$  and  $\zeta_2$  are the elevations of the incident and the scattered waves, we must have

$$\left(\frac{\partial \zeta_1}{\partial \xi} + \frac{\partial \zeta_2}{\partial \xi}\right)_{\xi=0} = 0. \quad (2)$$

The second boundary condition is

$$\zeta_2 \rightarrow 0 \text{ when } \xi \rightarrow +\infty, \quad (3)$$

since the influence of the plate-shape island is nil at infinity.

The equation (1) and the conditions (2), (3) are identical in form

with those in the case of the sound wave<sup>1)</sup>. Using the result of the sound wave, the elevation ( $\zeta_{\xi=0}$ ) of water at the surface of the plate is given as follows:

$$\zeta_{\xi=0} = (\zeta_1)_{\xi=0} + (\zeta_2)_{\xi=0}; \tag{4}$$

$$(\zeta_1)_{\xi=0} = 2e^{-i\omega t} \zeta_0 \sum_{n=0}^{\infty} \left[ \frac{A_0^{(2n)} ce_{2n}(\gamma) ce_{2n}(\theta)}{ce_{2n}\left(\frac{1}{2}\pi, q\right)} - \frac{ikA_1^{(2n+1)} ce_{2n+1}(\gamma) ce_{2n+1}(\theta)}{ce'_{2n+1}\left(\frac{1}{2}\pi, q\right)} \right]; \tag{5}$$

$$(\zeta_2)_{\xi=0} = 2e^{-i\omega t} \zeta_0 k \sum_{n=0}^{\infty} \left[ \frac{B_1^{(2n+1)} Ge y_{2n+1}(o) se_{2n+1}(\gamma) se_{2n+1}(\theta)}{N_{2n+1}^{(1)'}(o) se_{2n+1}\left(\frac{1}{2}\pi, q\right)} - \frac{ikB_2^{(2n+2)} Ge y_{2n+2}(o) se_{2n+2}(\gamma) se_{2n+2}(\theta)}{N_{2n+2}^{(1)'}(o) se'_{2n+2}\left(\frac{1}{2}\pi, q\right)} \right]; \tag{6}$$

$q = k^2$ ;  $A_0^{(2n)}$ ,  $A_1^{(2n+1)}$ ,  $B_1^{(2n+1)}$ ,  $B_2^{(2n+2)}$  are the coefficients of the first terms in Fourier expressions of the Mathieu functions  $ce_{2n}(\theta, q)$ ,  $ce_{2n+1}(\theta, q)$ ,  $se_{2n+1}(\theta, q)$ ,  $se_{2n+2}(\theta, q)$  respectively, i.e.,

$$\left. \begin{aligned} ce_{2n}(\theta, q) &= \sum_{r=0}^{\infty} A_{2r}^{(2n)} \cos 2r\theta \\ ce_{2n+1}(\theta, q) &= \sum_{r=0}^{\infty} A_{2r+1}^{(2n+1)} \cos (2r+1)\theta \\ se_{2n+1}(\theta, q) &= \sum_{r=0}^{\infty} B_{2r+1}^{(2n+1)} \sin (2r+1)\theta \\ se_{2n+2}(\theta, q) &= \sum_{r=0}^{\infty} B_{2r+2}^{(2n+2)} \sin (2r+2)\theta \end{aligned} \right\} \tag{7}$$

The first derivatives of the Mathieu functions in (5) and (6) are given from (7) as follows:-

$$\left. \begin{aligned} ce'_{2n+1}\left(\frac{\pi}{2}, q\right) &= \sum_{r=0}^{\infty} (-1)^{r+1} \cdot (2r+1) \cdot A_{2r+1}^{(2n+1)} \\ se'_{2n+2}\left(\frac{\pi}{2}, q\right) &= \sum_{r=0}^{\infty} (-1)^{r+1} \cdot (2r+2) \cdot B_{2r+2}^{(2n+2)} \end{aligned} \right\} \tag{8}$$

1) N. W. MCLACHLAN, *Theory and Application of Mathieu Functions* (Oxford, 1951), 362.

The modified Mathieu functions  $Ge_{2n+1}(Z)$ ,  $Ne_{2n+1}^{(1)}(Z)$ ,  $Ge_{2n+2}(Z)$  and  $Ne_{2n+2}^{(1)}(Z)$  have several kinds of expression in series. Since the values of the derivatives of these functions at zero point are dealt (refer to (5) and (6)), we must use the series of the Bessel function product which are uniformly and absolutely convergent in complex variable at such a critical point and hence these series can be differentiated term by term. Other series of single Bessel function are convergent at zero point, but not always "uniformly" convergent. Hence term-by-term differentiation of such non-product series is not guaranteed.

The Bessel function product series for  $Ge_{2n+1}(Z, q)$ ,  $Ge_{2n+2}(Z, q)$ ,  $Ne_{2n+1}^{(1)}(Z, q)$  and  $Ne_{2n+2}^{(1)}(Z, q)$  are given by MCLACHLAN<sup>2)</sup> as follows:-

$$\left. \begin{aligned} Ge_{2n+1}(Z, q) &= (s_{2n+1}/B_1^{(2n+1)}) \cdot \sum_{r=0}^{\infty} (-1)^r B_{2r+1}^{(2n+1)} [J_r(v_1) Y_{r+1}(v_2) - J_{r+1}(v_1) Y_r(v_2)] \\ Ge_{2n+2}(Z, q) &= -(s_{2n+2}/B_2^{(2n+2)}) \cdot \sum_{r=0}^{\infty} (-1)^r B_{2r+2}^{(2n+2)} [J_r(v_1) Y_{r+2}(v_2) - J_{r+2}(v_1) Y_r(v_2)] \\ Ne_{2n+1}^{(1)}(Z, q) &= (s_{2n+1}/B_1^{(2n+1)}) \cdot \sum_{r=0}^{\infty} (-1)^r B_{2r+1}^{(2n+1)} [J_r(v_1) H_{r+1}^{(1)}(v_2) - J_{r+1}(v_1) H_r^{(1)}(v_2)] \\ Ne_{2n+2}^{(1)}(Z, q) &= -(s_{2n+2}/B_2^{(2n+2)}) \cdot \sum_{r=0}^{\infty} (-1)^r B_{2r+2}^{(2n+2)} [J_r(v_1) H_{r+2}^{(1)}(v_2) - J_{r+2}(v_1) H_r^{(1)}(v_2)] \end{aligned} \right\} \quad (9)$$

where  $v_1 = ke^{-z}$  and  $v_2 = ke^{+z}$ .

After some calculation the above expressions (9) become

$$\left. \begin{aligned} \frac{Ge_{2n+1}(0, q)}{Ne_{2n+1}^{(1)'}(0, q)} &= \frac{\sum_{r=0}^{\infty} (-1)^r B_{2r+1}^{(2n+1)} P_r}{\sum_{r=0}^{\infty} (-1)^r B_{2r+1}^{(2n+1)} Q_r} \\ \frac{Ge_{2n+2}(0, q)}{Ne_{2n+2}^{(1)'}(0, q)} &= \frac{\sum_{r=0}^{\infty} (-1)^r B_{2r+2}^{(2n+2)} R_r}{\sum_{r=0}^{\infty} (-1)^r B_{2r+2}^{(2n+2)} T_r} \end{aligned} \right\} \quad (10)$$

where

$$P_r = J_r(1) \cdot Y_{r+1}(1) - J_{r+1}(1) \cdot Y_r(1),$$

2) N. W. MCLACHLAN, *Theory and Application of Mathieu Functions* (Oxford, 1951), 247 and 251.

$$\begin{aligned}
Q_r &= \frac{1}{2} [-J_{r-1}(1) \cdot H_{r+1}^{(1)}(1) - J_r(1) \cdot H_{r+2}^{(1)}(1) \\
&\quad - J_{r+1}(1) \cdot H_{r-1}^{(1)}(1) - J_{r+2}(1) \cdot H_r^{(1)}(1) \\
&\quad + 2\{J_r(1) \cdot H_r^{(1)}(1) + J_{r+1}(1) H_{r+1}^{(1)}(1)\}], \\
R_r &= J_r(1) \cdot Y_{r+2}(1) - J_{r+2}(1) Y_r(1), \\
T_r &= \frac{1}{2} [-J_{r-1}(1) - J_{r+1}(1)] \cdot H_{r+2}^{(1)}(1) \\
&\quad + J_r(1) \cdot \{H_{r+1}^{(1)}(1) - H_{r+3}^{(1)}(1)\} \\
&\quad + \{J_{r+1}(1) - J_{r+3}(1)\} \cdot H_r^{(1)}(1) \\
&\quad - J_{r+2}(1) \cdot \{H_{r-1}^{(1)}(1) - H_{r+1}^{(1)}(1)\}.
\end{aligned}$$

The values of the Mathieu functions  $ce_{2n}(\gamma)$ ,  $ce_{2n}(\theta)$ ,  $ce_{2n}(\pi/2, q)$ ,  $ce_{2n+1}(\gamma)$ ,  $ce_{2n+1}(\theta)$ ,  $se_{2n+1}(\gamma)$ ,  $se_{2n+1}(\theta)$ ,  $se_{2n+2}(\gamma)$ ,  $se_{2n+2}(\theta)$ ,  $se_{2n+1}(\pi/2, q)$  and the coefficients of the first terms of the Mathieu functions  $\{ce_{2n}(\gamma)$ ,  $ce_{2n+1}(\gamma)$ ,  $se_{2n+1}(\gamma)$ ,  $se_{2n+2}(\gamma)\}$  in Fourier expressions— $A_0^{(2n)}$ ,  $A_1^{(2n+1)}$ ,  $B_1^{(2n+1)}$ ,  $B_2^{(2n+2)}$ — are given in a table by Ince<sup>3)</sup>.

In order to see the nature of diffraction of the Chilean Tsunami around the island of Amami-Oshima, we have considered the following model:-

(1) Amami-Oshima is replaced by a plate with length 60 Km ( $=2h$ ) and (2) the depth of the sea is everywhere 200 m ( $=H$ ).

Then the Chilean Tsunami of 1960 may be considered to impinge on the island at the angle of  $\theta=130^\circ$  (refer to Fig. 1).

When the depth of the sea is 200 m, the velocity of long wave ( $c$ ) becomes 44.27 m/s ( $=\sqrt{gH}$ ;  $g=9.8 \text{ m/s}^2$ ). The marigram recorded at Kikaigashima near Amami-Oshima shows that the period of the Chilean Tsunami of 1960 is about 35 minutes<sup>4)</sup>. Therefore, the wave-length ( $\lambda$ ) of the invading tsunami is 94.248 Km ( $=cT$ ;  $c=44.24 \text{ m/s}$ ,  $T=35 \text{ min.}$ ). Thus the value of  $q$  contained in the Mathieu and the modified Mathieu functions becomes  $1(=k^2=(k_1 h/2)^2=(\omega h/2c)^2=(\pi h/\lambda)^2)$ ;  $h=30 \text{ Km}$ ,  $\lambda=94.248 \text{ Km}$ ).

Substituting  $q=1$  and  $\theta=130^\circ$  in (4), (5), (6), (7) (8), (9), and (10),

3) E. L. INCE, "Tables of the Elliptic-cylinder Functions", *Proc. Roy. Soc. Edinb.*, 52 (1931-32), 355.

4) Report on the Chilean Tsunami of May 24, 1960, as observed along the Coast of Japan, 393.

and using Ince's Table<sup>5)</sup> and the Table of Bessel Function<sup>6)</sup>, the expressions (5) and (6) are reduced to simple forms given below:-

$$(\zeta_1)_{\xi=0} = 2e^{-i\omega t} \zeta_0 \cdot \sum_{n=0}^{\infty} [U_{2n}^{(c)} c e_{2n}(\gamma) + V_{2n+1}^{(c)} c e_{2n+1}(\gamma)], \quad (11)$$

$$(\zeta_2)_{\xi=0} = 2e^{-i\omega t} \zeta_0 \cdot \sum_{n=0}^{\infty} [U_{2n+1}^{(s)} s e_{2n+1}(\gamma) + V_{2n+2}^{(s)} s e_{2n+2}(\gamma)], \quad (12)$$

where  $U_{2n}^{(c)}$ ,  $V_{2n+1}^{(c)}$ ,  $U_{2n+1}^{(s)}$ ,  $V_{2n+2}^{(s)}$  ( $n=0, 1, 2$ ) are tabulated in Table I.

Table I. The values of  $U_{2n}^{(c)}$ ,  $V_{2n+1}^{(c)}$ ,  $U_{2n+1}^{(s)}$ , and  $V_{2n+2}^{(s)}$ .

| n | $U_{2n}^{(c)}$ | $V_{2n+1}^{(c)}$ | $U_{2n+1}^{(s)}$     | $V_{2n+2}^{(s)}$     |
|---|----------------|------------------|----------------------|----------------------|
| 0 | +0.47749       | - i 0.51932      | -0.48086 + i 0.09215 | +0.31861 + i 0.07100 |
| 1 | -0.03466       | - i 0.03298      | +0.00023 - i 0.02861 | +0.00116 + i 0.00000 |
| 2 | -0.00522       | + i 0.00023      | +0.00000 - i 0.00048 | -0.00004 + i 0.00000 |

Table II. The relative amplitude  $|\zeta|/\zeta_0$  around the plate.

| $\eta^\circ$ | $x = h \cdot \cos \eta$ (km)<br>(the upper side of the plate) | $ \zeta /\zeta_0$ |
|--------------|---|-------------------|
| 0°           | +30.000   | +1.00000          |
| 20°          | +28.191   | +0.97930          |
| 40°          | +22.981   | +0.91324          |
| 60°          | +15.000   | +0.65344          |
| 80°          | + 5.210   | +0.19059          |
| 90°          | 0   | +0.27384          |
| 100°         | - 5.210   | +0.52718          |
| 120°         | -15.000   | +0.87304          |
| 140°         | -22.981   | +0.93906          |
| 150°         | -25.981   | +0.91074          |
| 160°         | -28.191   | +0.88746          |
| 180°         | -30.000   | +1.00000          |

| $\eta^\circ$ | $x = h \cdot \cos \eta$ (km)<br>(the lower side of the plate) | $ \zeta /\zeta_0$ |
|--------------|---|-------------------|
| 360°         | +30.000   | +1.00000          |
| 340°         | +28.191   | +1.0382           |
| 320°         | +22.981   | +1.1162           |
| 300°         | +15.000   | +1.3595           |
| 280°         | + 5.210   | +1.8511           |

5) E. L. INCE, *loc. cit.*, 3).

6) G. N. WATSON, *Theory of Bessel Functions* (Cambridge, 1922).

At the surface of the plate the relation between the Cartesian and the elliptic coordinates,  $x=h \cdot \cosh \zeta \cdot \cos \eta$  and  $y=h \cdot \sinh \xi \cdot \sin \eta$ , becomes

$$\left. \begin{aligned} x &= h \cdot \cos \eta & (2\pi > \eta \geq 0) \\ y &= 0 \end{aligned} \right\}, \quad (13)$$

so that by use of (11), (12), (13) and Ince's Table<sup>7)</sup> the resultant elevation of water at the surface of the plate —(4)— is known. The result of the numerical computation is given in Table II, whose graphs are shown in Figs. 3 and 4. For convenience of expression "relative amplitude", which is defined by  $|\zeta|/\zeta_0$ , is introduced.

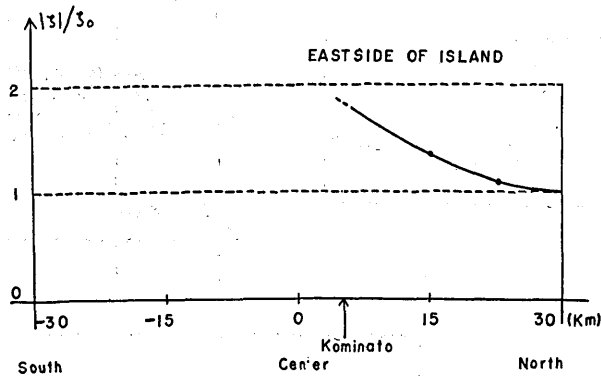


Fig. 3.

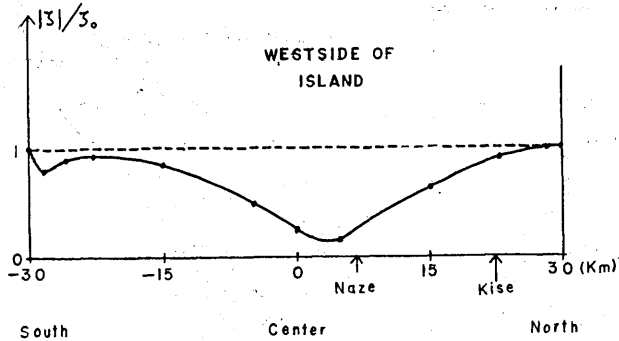


Fig. 4.

#### 4. Explanation of the Chilean Tsunami at Amami-Ōshima.

##### 4.1. The northern part of the island (Yō and Kasari).

From the refraction diagram (Fig. 1) we can expect high waves in

7) E. L. INCE, *loc. cit.*, 3).

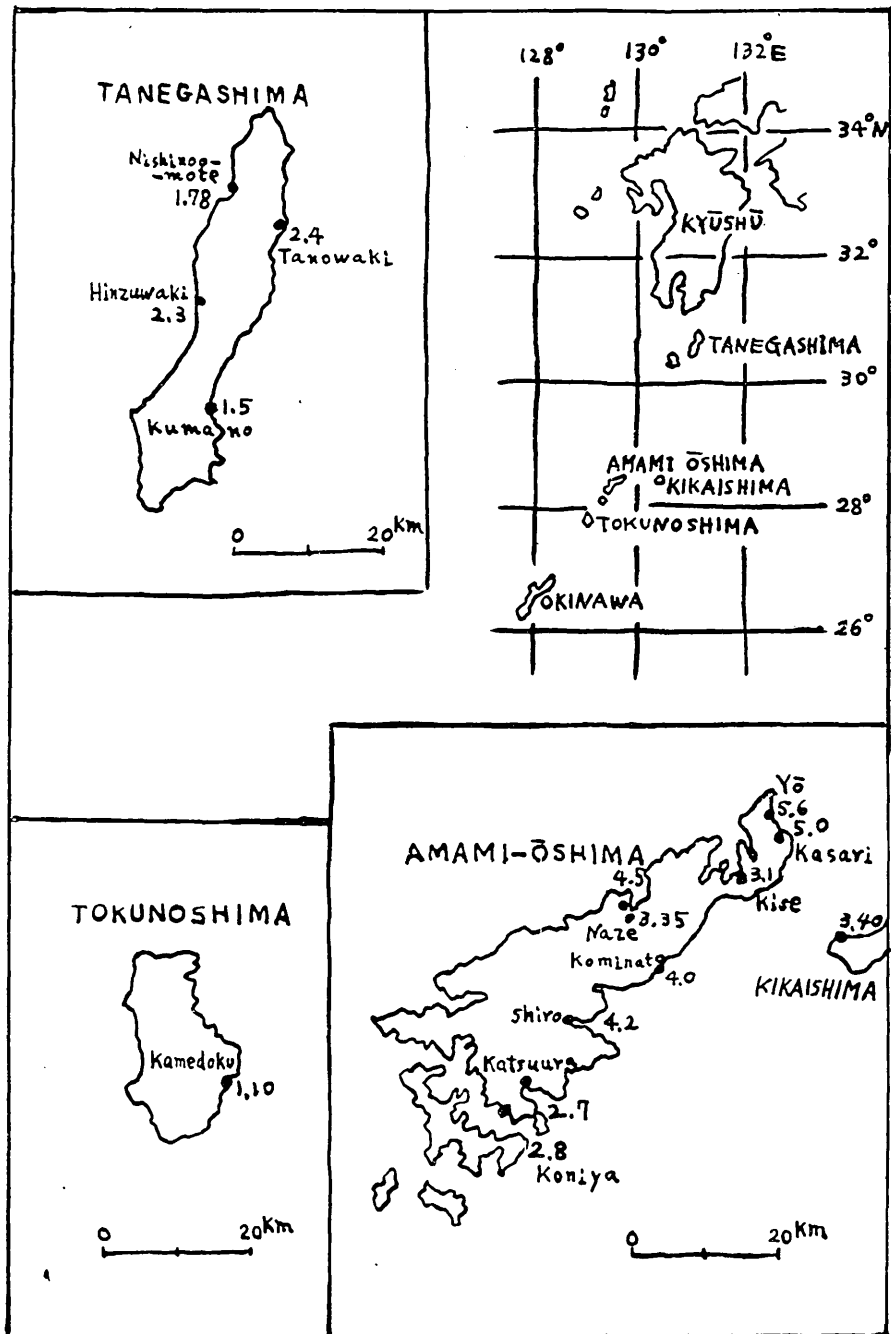


Fig. 5.



the northern part of the island. Actually the inundation height of the Chilean Tsunami of 1960 observed in the northern part of Amami-Oshima was remarkably higher than in the southern part of the island and nearby islands (Fig. 5).<sup>8)</sup>

4.2. The eastside of the central part of the island (Kominato and Shiro).

The refraction diagram (Fig. 1) shows that the waves diverge in this part, while in the southern part of the island the wave front runs parallel to the coastline and the wave height of the Chilean Tsunami of 1960 was about 2.7 m. Hence we cannot expect such high waves as 4.0 m in the central part of the island on the occasion of the Chilean Tsunami. A possible explanation for this phenomenon may be the flowing (or diffracting) of the waves along the plate, which is shown in Fig. 3.

4.3. The northwestern part of the island (Kise and Naze).

The wave heights at Yō and Kasari in the most northern part are twice that of the incident wave by reflection so the amplitude of the incident wave is about 2.3 m. Therefore, from Fig. 4 the expected wave heights at Kise and Naze are 2.07 m ( $=2.3 \times 0.9$  m) and 0.46 m ( $=2.3 \times 0.2$  m) respectively, which cannot explain the extra-ordinarily high waves 3.1 m (at Kise) and 3.35~4.0 m (at Naze) of the Chilean Tsunami. Also the refraction diagram (Fig. 1) does not show any convergence of the waves. Thus we may conclude that the high waves at Kise and Naze may be attributed to the seiches of each bay or that the model of the plate must be modified to a more suitable one. These considerations will be made in the near future.

### 5. Acknowledgment

The author is indebted to Professor R. Takahasi and Assistant Professor K. Kajiura of this Institute for their helpful discussions.

### 3. 奄美大島における1960年5月24日の津波

地震研究所 桃井高夫

日本の南端に位する奄美大島は1960年のチリ津波のとき、周辺の島々に比べて異常な波高を記録した。筆者は奄美大島周辺におけるチリ津波の refraction diagram をかき、また、奄美大島を、長さ60 Kmの板によつておきかえ、その回りの波の回折を計算してチリ津波の異常波高の説明を試みた。その結果島の北端と中部の東岸の異常波高は一応定性的に説明がいついたが、北東部の湾内の異常波高は説明できなかつた。

8) Report on the Chilean Tsunami, loc. cit., 4), 200.